Untargeted Metabolomics Reveals Species-Specific Metabolite Production and Shared Nutrient Consumption by *Pseudomonas aeruginosa* and *Staphylococcus aureus*

Laura J. Dunphy,[a] Kassandra L. Grimes,[b] Nishikant Wase,[c] Glynis L. Kolling,[a,d] Jason A. Papin[a,d,e]

[a]Department of Biomedical Engineering, University of Virginia, Charlottesville, Virginia, USA
[b]Department of Engineering Systems and Environment, University of Virginia, Charlottesville, Virginia, USA
[c]Biomolecular Analysis Facility, School of Medicine, University of Virginia, Charlottesville, Virginia, USA
[d]Division of Infectious Diseases and International Health, Department of Medicine, University of Virginia, Charlottesville, Virginia, USA
[e]Department of Biochemistry and Molecular Genetics, University of Virginia, Charlottesville, Virginia, USA

ABSTRACT While bacterial metabolism is known to impact antibiotic efficacy and virulence, the metabolic capacities of individual microbes in cystic fibrosis lung infections are difficult to disentangle from sputum samples. Here, we show that untargeted metabolomic profiling of supernatants of multiple strains of *Pseudomonas aeruginosa* and *Staphylococcus aureus* grown in monoculture in synthetic cystic fibrosis media (SCFM) reveals distinct species-specific metabolic signatures despite intraspecies metabolic variability. We identify a set of 15 metabolites that were significantly consumed by both *P. aeruginosa* and *S. aureus*, suggesting that nutrient competition has the potential to impact community dynamics even in the absence of other pathogen-pathogen interactions. Finally, metabolites that were uniquely produced by one species or the other were identified. Specifically, the virulence factor precursor anthranilic acid, as well as the quinoline 2,4-quinolinediol (DHQ), were robustly produced across all tested strains of *P. aeruginosa*. Through the direct comparison of the extracellular metabolism of *P. aeruginosa* and *S. aureus* in a physiologically relevant environment, this work provides insight toward the potential for metabolic interactions *in vivo* and supports the development of species-specific diagnostic markers of infection.

IMPORTANCE Interactions between *P. aeruginosa* and *S. aureus* can impact pathogenicity and antimicrobial efficacy. In this study, we aim to better understand the potential for metabolic interactions between *P. aeruginosa* and *S. aureus* in an environment resembling the cystic fibrosis lung. We find that *S. aureus* and *P. aeruginosa* consume many of the same nutrients, suggesting that metabolic competition may play an important role in community dynamics during coinfection. We further identify metabolites uniquely produced by either organism with the potential to be developed into species-specific biomarkers of infection in the cystic fibrosis lung.

KEYWORDS LC-MS, metabolism, *Pseudomonas aeruginosa*, *Staphylococcus aureus*

*P*seudomonas aeruginosa and *Staphylococcus aureus* are opportunistic pathogens that commonly infect the lungs of patients with cystic fibrosis (CF) (1–3). Coinfection with both pathogens, particularly *P. aeruginosa* and methicillin-resistant *S. aureus* (MRSA), has been associated with worsened patient outcomes (2, 4, 5). Both antagonistic and synergistic interactions have been observed between *P. aeruginosa* and *S. aureus* (2, 6). For example, *P. aeruginosa* can produce the virulence factor 2-heptyl-4-hydroxyquinoline *N*-oxide (HQNO), which inhibits *S. aureus* growth and drives *S. aureus* into a fermentative metabolic state (7, 8) but consequently decreases the susceptibility of *S. aureus* to multiple antimicrobials (9, 10). While *S. aureus* dominates CF

lung infections early in life, *P. aeruginosa* tends to take over as patients age, often accompanied by worsening lung function (1, 3, 11). Continued understanding of interactions and population dynamics between these two pathogens is likely to result in improved therapeutic strategies and control of chronic infection in the CF lung.

Metabolomics profiling is increasingly being applied as a method to study polymicrobial communities (12–15) and to identify *in vivo* biomarkers of infection (16–19). Metabolomics profiling of sputum samples has enabled the identification of host-derived markers of CF (20); however, the high degree of metabolic and microbial heterogeneity across sputum samples makes it difficult to deconvolute the metabolic contributions of individual microbial species (20, 21). Alternatively, *P. aeruginosa* grown in the defined physiologically relevant media, synthetic cystic fibrosis media (SCFM), exhibits a transcriptional program similar to *P. aeruginosa* grown in CF sputum (22), providing a more reproducible way to study and compare the primary metabolism of individual species and strains. *In vitro* metabolomic profiling has enabled an improved understanding of *P. aeruginosa* metabolism as a function of altered media environments (23, 24), heterogeneous environmental backgrounds (25), variable antimicrobial resistance and virulence profiles (26), and coculture with *S. aureus* (15). While others have profiled the metabolome of *P. aeruginosa* (15, 23–27), to our knowledge, there are no open-source untargeted metabolomics data sets of multiple strains of both *P. aeruginosa* and *S. aureus* grown independently in a lung-like medium. Despite appreciated discrepancies between *in vitro* and *in vivo* metabolomics profiles (20), identification of robust cross-strain metabolic profiles for *P. aeruginosa* and *S. aureus* may help to guide the clinical study of pathogen-pathogen interactions and selection of candidate biomarkers of infection.

Here, we profiled the metabolism of multiple strains of *P. aeruginosa* and *S. aureus* grown in monoculture in SCFM (22). We show from untargeted metabolomics of culture supernatant that each species had a distinct metabolic signature despite strain-to-strain differences in significantly consumed or produced metabolites. We further compared metabolite consumption across species and found that *P. aeruginosa* and *S. aureus* robustly consume a shared subset of 15 nutrients. This result suggests that, even in the absence of *P. aeruginosa*-mediated growth inhibition and killing, *S. aureus* may be required to compete with *P. aeruginosa* for key nutrients in coculture. This result is consistent with the previous observation that coexistence between *P. aeruginosa* and *S. aureus* in brain heart infusion (BHI) was associated with a transcriptional shift away from glucose metabolism in *S. aureus* (28). Finally, we identify metabolites uniquely produced by each species across all tested strains. Together, our findings provide new insight into the capacity for competitive metabolic interaction between *P. aeruginosa* and *S. aureus* and suggest species-specific biomarkers of infection with the potential to improve treatment and diagnosis of CF lung infections.

RESULTS

Untargeted metabolomics of *P. aeruginosa* and *S. aureus* in monoculture in a lung-like media. Five strains of *P. aeruginosa* and four strains of *S. aureus* were grown individually in monoculture in SCFM (Fig. 1A). The strains came from various sources (e.g., laboratory, clinical) and genetic backgrounds and displayed various levels of antimicrobial susceptibility and pigment production (Table 1; Fig. 1B to E; Fig. S1 in the supplemental material). *P. aeruginosa* strain UCBPP-PA14 was profiled both before (isogenic) and after (SCFM evolved) 10 days of laboratory adaptation to SCFM (Fig. S2; see Materials and Methods). This was done to evaluate the sensitivity of *P. aeruginosa* metabolism to heterogeneous recent environmental backgrounds. Additionally, the *S. aureus* laboratory strains ATCC 29213 (methicillin sensitive) and USA300 LAC (methicillin resistant) and five isolates from the CDC and FDA Antibiotic Resistance Isolate Bank (29; https://www.cdc.gov/drugresistance/resistance-bank/index.html) were selected (Table 1). Interestingly, strains with highly similar genomes could display dissimilar antimicrobial susceptibility profiles (Fig. 1B to E). Untargeted metabolomics data were
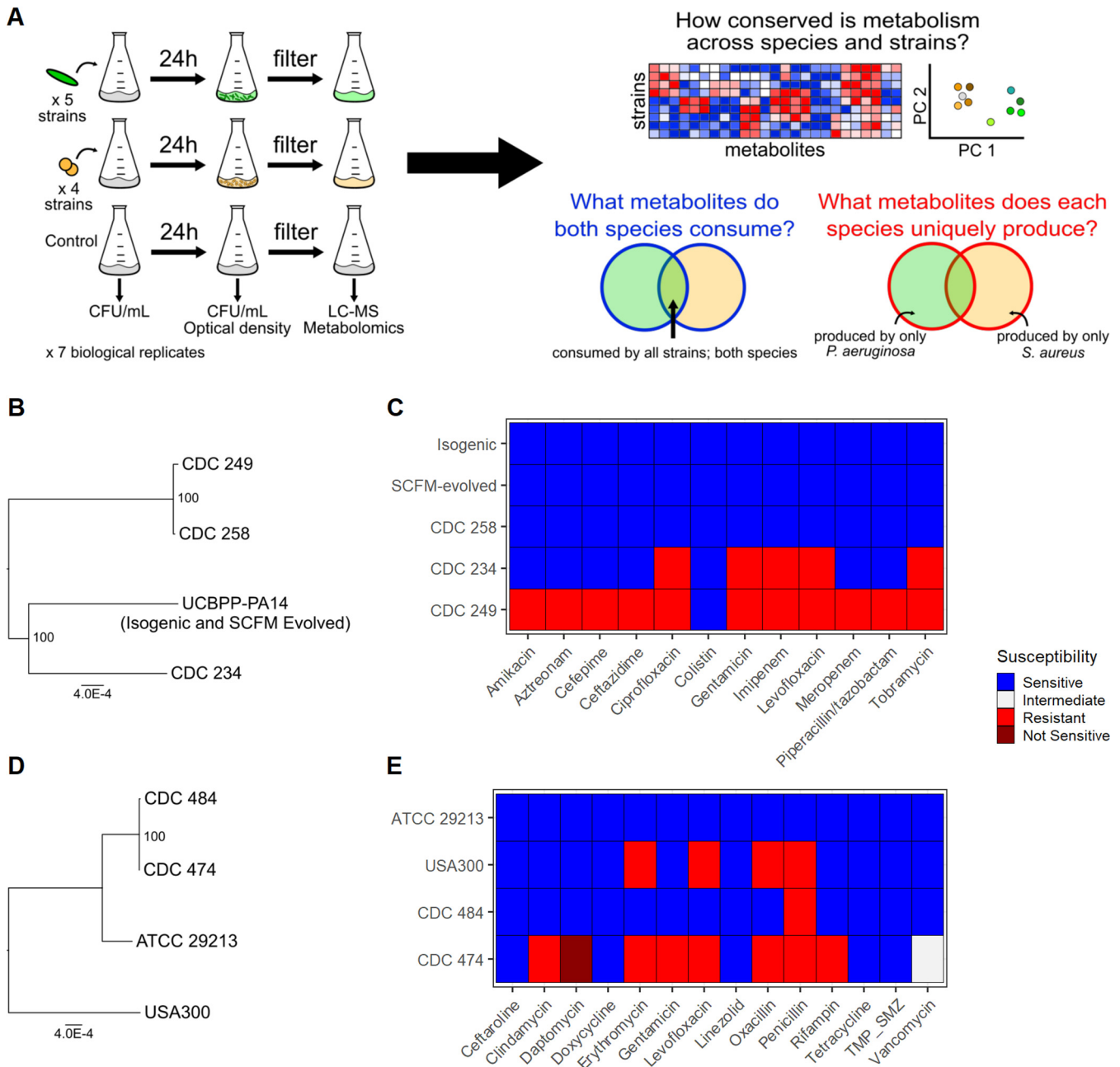
FIG 1 Summary of experimental design and bacterial strains used in this study. (A) Five strains of *P. aeruginosa* (green) and four strains of *S. aureus* (yellow) were each grown individually in SCFM for 24 h. Cultures were filter sterilized, and LC-MS was performed on supernatants. SCFM medium was also profiled as a control. Strain-specific metabolic profiles, cross-species metabolite consumption, and species-specific metabolite production were identified. (B and D) Phylogenetic trees of *P. aeruginosa* (B) and *S. aureus* (D) strains. Reference genomes were used for laboratory strains UCBPP-PA14, ATCC 29213, and USA300. A single reference genome was used for isogenic and SCFM-evolved UCBPP-PA14 given their shared history and highly similar metabolic functionality. (C and E) Antimicrobial susceptibility profiles of *P. aeruginosa* (C) and *S. aureus* (E) strains.

generated from the supernatant of each strain and compared to unconditioned media to evaluate strain- and species-specific metabolite consumption and production.

Out of 314 metabolites identified by untargeted metabolomics, 288 were significantly altered ($P < 0.05$) in the supernatant of at least one strain relative to unconditioned media. *P. aeruginosa* strains exhibited generally higher log$_2$ fold change (log$_2$FC) than *S. aureus* strains in significantly consumed or produced metabolites (Fig. 2A). Additionally, clustering the raw peak areas of all 314 identified metabolites with principal coordinate analysis (PCoA) revealed that *P. aeruginosa* strains were distinct from *S. aureus* profiles, which were relatively similar to unconditioned SCFM

TABLE 1 Laboratory strains and clinical isolates used in this study

Identifier	Species	Strain	Sequence (accession no.)	Reference or source
Isogenic	*P. aeruginosa*	UCBPP-PA14	GenBank accession no. NC_008463.1	47, 57
SCFM evolved	*P. aeruginosa*	Adapted UCBPP-PA14	GenBank accession no. NC_008463.1	This study (Materials and Methods), 57[a]
CDC258	*P. aeruginosa*	Clinical	SRA accession no. SRR4417541	29
CDC234	*P. aeruginosa*	Clinical	SRA accession no. SRR4417559	29
CDC249	*P. aeruginosa*	Clinical	SRA accession no. SRR5122332	29
ATCC 29213	*S. aureus*	ATCC 29213	Assembly accession no. GCF_001267715.1	58, 59[a]
USA300	*S. aureus*	USA300 LAC	GenBank accession no. NC_007793.1	This study (Acknowledgments), 60[a]
CDC484	*S. aureus*	Clinical	SRA accession no. SRR8526670	29
CDC474	*S. aureus*	Clinical	SRA accession no. SRR6985717	29

[a]Source of sequence data if different from source of isolate (e.g., reference genome).

controls (Fig. 2B). Both of these results corresponded with the observation that *P. aeruginosa* strains grew to higher culture densities than *S. aureus* strains in SCFM (Fig. S3). Individual clustering of each species further highlighted strain-specific differences in *P. aeruginosa* metabolomes (Fig. 2C), while no clear strain-specific profiles emerged in *S. aureus* metabolomes (Fig. 2D). These results demonstrate the ability of each pathogen to alter the metabolic landscape of a lung-like environment.

Metabolite production and consumption were mostly conserved across strains of the same species. Overlap between intraspecies extracellular metabolomes was evaluated to identify robust species-specific metabolic signatures and assess strain-to-strain metabolic variability (Fig. 3). For the five strains of *P. aeruginosa*, the majority of metabolites produced (131 metabolites, $P < 0.05$, $\log_2 FC > 0$) and consumed (49 metabolites, $P < 0.05$, $\log_2 FC < 0$) were conserved (Fig. 3A and B). Metabolism was highly similar between the isogenic and SCFM-evolved strains (235/256 metabolites, $P < 0.05$), indicating that prior adaptation to SCFM did not have a strong impact on metabolite consumption or production.

Similar to what was seen in *P. aeruginosa*, the majority of metabolites produced by *S. aureus* (54 metabolites, $P < 0.05$, $\log_2 FC > 0$) were produced by all four strains (Fig. 3C). *S. aureus* strains reached lower final growth densities than *P. aeruginosa* strains (Fig. S3), and metabolite consumption by *S. aureus* was more variable, with 18 conserved metabolites and 19 metabolites only consumed by subsets of the four strains (Fig. 3D). Overall, we observed a high degree of consistency across metabolites significantly consumed and produced by strains of the same species, highlighting a shared core metabolic program in a CF lung-like environment. Intraspecies differences in metabolism additionally suggest the potential for less robust, strain-specific metabolic interactions between *P. aeruginosa* and *S. aureus*.

A subset of metabolites was robustly consumed by both *P. aeruginosa* and *S. aureus*. In order to predict nutrients that *P. aeruginosa* and *S. aureus* may compete over when colocalized in the lung or *in vitro*, metabolite consumption was compared across all strains of each species. Metabolomics data revealed 15 metabolites significantly consumed ($P < 0.05$, $\log_2 FC < 0$) by all nine profiled strains (Fig. 4A), indicating that the majority of metabolites robustly consumed by *S. aureus* were also robustly consumed by *P. aeruginosa*. These metabolites included several key amino acids (e.g., tryptophan, L-serine, L-glutamic acid, and ornithine) and lactic acid (Fig. 4B and C). Additionally, all nine strains also consumed glucose from the media (Fig. S4). These results suggest that in addition to direct suppression of *S. aureus* growth by *P. aeruginosa* (6, 8, 30), *P. aeruginosa* and *S. aureus* have the potential to metabolically compete over key nutrients when cocultured in a lung-like media.

Robust species-specific-produced metabolites are potential biomarkers of lung infection. Metabolites that are produced uniquely by a single species have the potential to be developed into biomarkers of *P. aeruginosa* or *S. aureus* infection. In total, there were 84 metabolites that were statistically significantly ($P < 0.05$, $\log_2 FC > 0$) produced by all five strains of *P. aeruginosa* and not produced by *S. aureus*. Conversely, there were 15 metabolites produced uniquely by all four strains of *S. aureus* (Fig. 5A). In an effort to account for potential noise of the environmental milieu, only
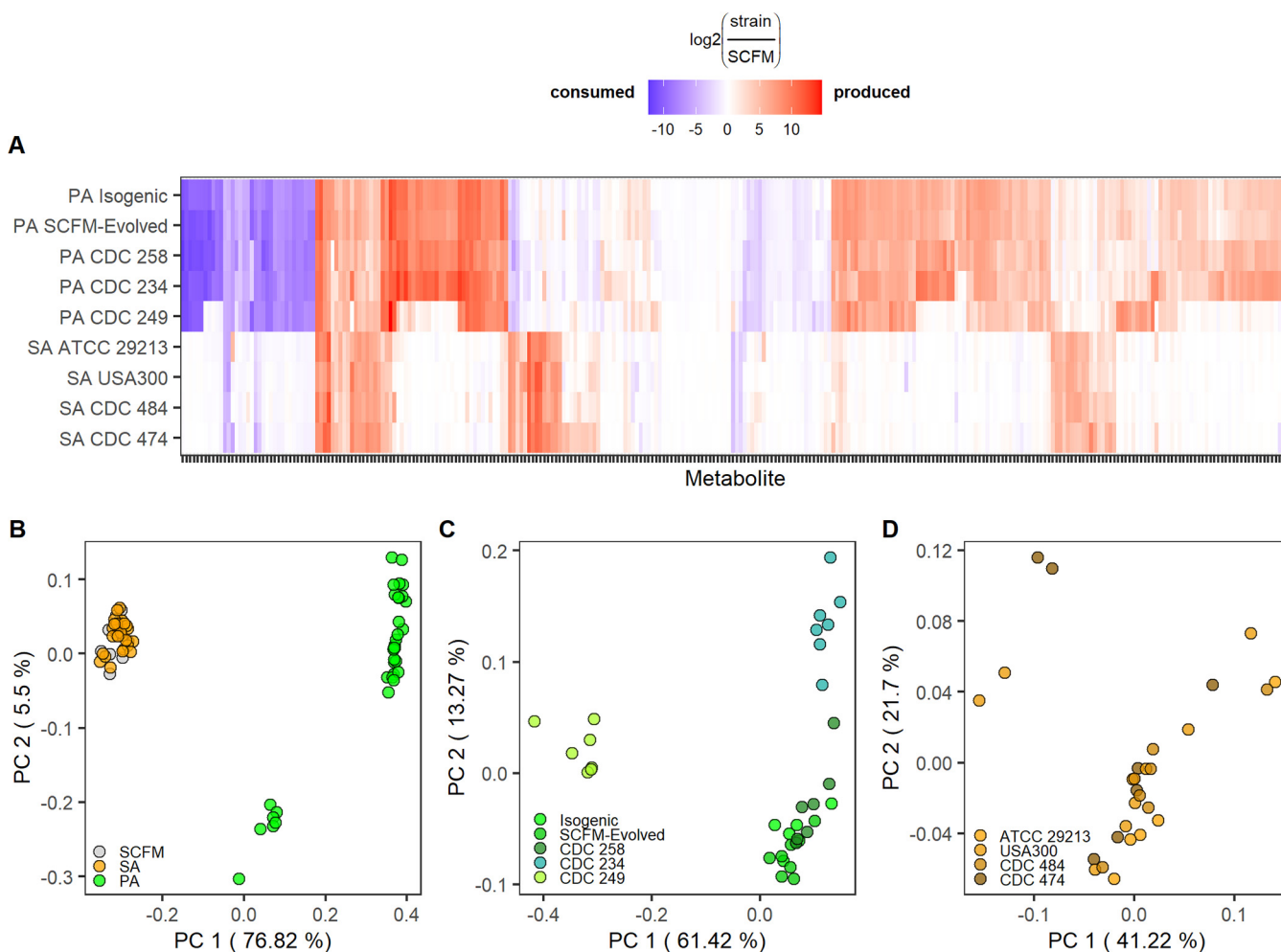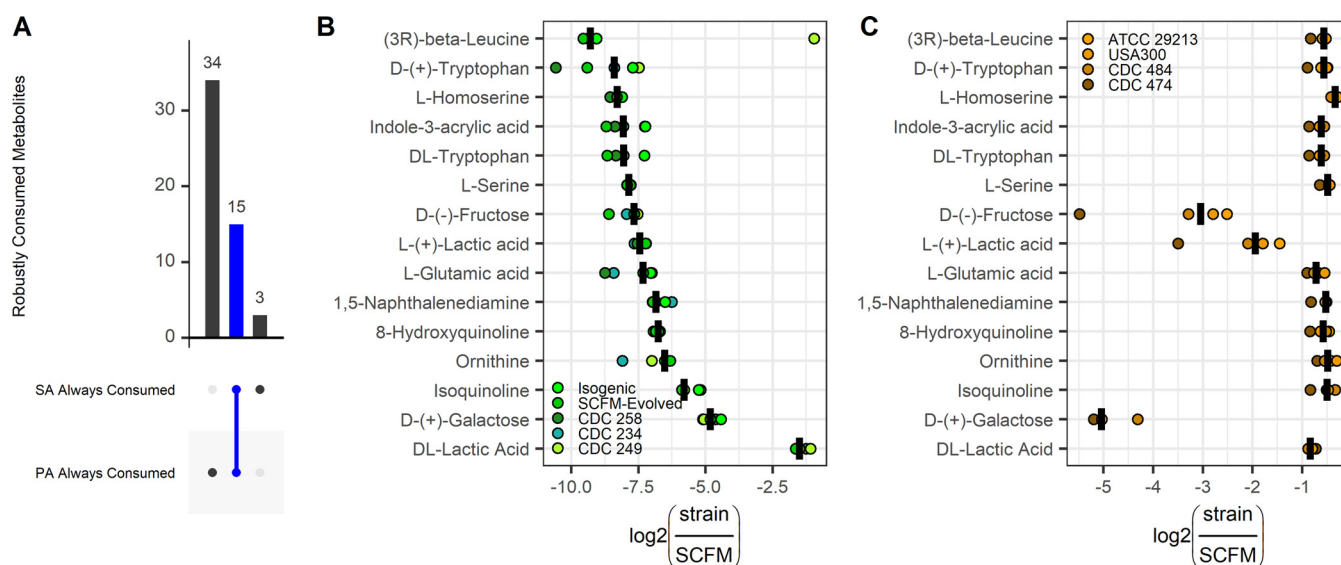
FIG 2 Metabolic profiles of *P. aeruginosa* and *S. aureus* grown in monoculture in SCFM. (A) Metabolomics profiles of conditioned SCFM. Metabolites significantly altered relative to SCFM in at least one condition are shown ($P < 0.05$). Metabolites clustered by Euclidean distance with complete linkage. Significance determined by Wilcoxon rank sum test with Benjamini-Hochberg correction. (B to D) PCoA of Bray-Curtis distances calculated using all raw peak areas for all replicates of all strains (B), raw peak areas for *P. aeruginosa* strains only (C), or *S. aureus* strains only (D). Percent variance is shown for each principal coordinate. $n = 7$ replicates for all conditions.

significantly altered metabolites with a minimum $\log_2$FC of >1 across all strains of each species are shown (Fig. 5B and C; Data Set S1).

Metabolites produced uniquely by *P. aeruginosa* relative to unconditioned SCFM included nucleic acids and amino acids, their derivatives, as well as a downstream quinoline from the *Pseudomonas* quinolone signal (PQS) system (31) (Fig. 5B). Anthranilic acid and kynurenic acid, known downstream products of tryptophan metabolism (32), were both highly produced ($\log_2$FC > 5) in *P. aeruginosa*-conditioned SCFM supernatants. Downstream metabolites of several amino acids, including nicotinamide, nicotinic acid, and the *P. aeruginosa*-specific metabolite 6-hydroxynicotinc acid (33), were also increased. Although these metabolites were not seen in *S. aureus*-conditioned SCFM supernatants, more research is required to determine whether they are unique to *P. aeruginosa* and can be distinguished from the host milieu. Interestingly, the metabolite, 2,4-quinolinediol (DHQ), which has been shown to increase virulence and maintain pyocyanin production in model organisms (31), was highly elevated in supernatants of all five tested strains of *P. aeruginosa*. DHQ has been measured in CF sputum samples (31), suggesting that it has the potential to be a strong candidate biomarker for *P. aeruginosa* lung infection.

Although *S. aureus* did not grow as robustly in SCFM as *P. aeruginosa*, all four strains produced a shared set of 54 metabolites (Fig. 3C), 15 of which were not significantly

FIG 3 Intraspecies strain-specific metabolite production and consumption. Number of significant metabolites produced ($P < 0.05$, $\log_2 FC > 0$) or consumed ($P < 0.05$, $\log_2 FC < 0$) by subsets of *P. aeruginosa* strains (A and B) or *S. aureus* strains (C and D). Metabolites produced by all strains of a species are shown in red. Metabolites consumed by all strains of a species are shown in blue.

produced by any strains of *P. aeruginosa* (Fig. 5A). *S. aureus* produced fewer unique metabolites than *P. aeruginosa*, and these metabolites consisted mostly of glycolysis or tricarboxylic acid (TCA) cycle components and their derivatives (Fig. 5C). The metabolite with the largest fold change from unconditioned media, 2-oxoglutaric acid, is known to be produced during catabolism of L-glutamic acid and other amino acids (34). We hypothesize that these components were secreted following amino acid degradation and not consumed because other preferred carbon sources were still freely available (35). Consequently, it is unclear whether these metabolites would remain available in the host milieu or whether they would be taken up by *S. aureus* in the absence of glucose or by other microbes or the host. For example, it has been previously shown that *P. aeruginosa* is capable of catabolizing citric acid (36). We conclude that while *S. aureus* produces metabolites that *P. aeruginosa* does not, known *S. aureus*-specific proteins (e.g., hemolysins) may be more robust and unique biomarkers of *S. aureus* infection in sputum. It is worth noting, however, that *S. aureus* has been shown to produce fewer virulence factors *in vitro* than in CF sputum (37).

DISCUSSION

Here, we have shown that *P. aeruginosa* and *S. aureus* have distinct metabolomes, with the majority of significantly altered metabolites conserved within strains of each species (Fig. 3). We further identified a subset of 15 metabolites that were significantly consumed by both species, including the known sputum components L-lactic acid, L-glutamic acid, L-serine, DL-tryptophan, and ornithine (Fig. 4) (22). Glucose was additionally consumed by all strains (Fig. S4). These robustly consumed metabolites suggest a baseline level of nutrient competition between *P. aeruginosa* and *S. aureus* in a

FIG 4 Shared metabolite consumption between *P. aeruginosa* and *S. aureus* in a lung-like medium. (A) Number of significant metabolites robustly consumed across all tested monocultures of *P. aeruginosa* and *S. aureus* ($P < 0.05$, $\log_2 FC < 0$). $\log_2 FCs$ in metabolites consumed by both *P. aeruginosa* (B) and *S. aureus* (C) relative to SCFM. Crossbar denotes median change across strains.

CF lung-like environment. Finally, metabolites are increasingly being considered biomarkers of infection (16–19), and here, we proposed a subset of produced metabolites involved in L-tryptophan catabolism and PQS signaling as potential unique biomarkers of *P. aeruginosa* infection in the CF lung (Fig. 5B).

Although *P. aeruginosa* and *S. aureus* are known to coinfect the lung, *in vitro* cocultures of these two organisms can be difficult to maintain (8, 38). In addition to known mechanisms of hostility of *P. aeruginosa* toward *S. aureus* to directly kill or drive *S. aureus* into a less metabolically active state (2), we propose that *P. aeruginosa* and *S. aureus* coculture may be further complicated by the versatile nature of *P. aeruginosa* catabolism. In addition to the 15 metabolites consumed by all strains of both species, *P. aeruginosa* robustly consumed another 34 metabolites (Fig. 4), indicating that, barring any condition-specific or coculture-driven shifts in carbon source catabolism (39), there may be few nutrients uniquely available to *S. aureus* in coculture. Given the large overlap in metabolite consumption, we hypothesize that it may be unlikely that *P. aeruginosa* and non-small colony variants of *S. aureus* stably colocalize closely enough in the CF lung to impact one another's nutrient environments. That said, adaptation to ciprofloxacin exposure has been shown to result in a loss of catabolic function in *P. aeruginosa* (36), and therefore, treatment-driven catabolic deficits may lessen the potential for nutrient competition and promote coexistence of the two pathogens *in vivo*.

P. aeruginosa-conditioned SCFM contained molecules known to be involved in PQS signaling and virulence. Specifically, anthranilic acid, a precursor of quinoline signaling (40, 41), and the quinoline DHQ (31, 42) were consistently detected in the supernatant of all five strains (Fig. 5B). Anthranilic acid is an important precursor and suggested therapeutic target for PQS signaling and can be derived from L-tryptophan catabolism or chorismate (32, 43, 44). Consumption of L-tryptophan (Fig. 4B) and production of kynurenic acid (Fig. 5B), another product of L-tryptophan catabolism (32), suggest that L-tryptophan was the main precursor of anthranilic acid in the conditioned SCFM, consistent with literature that this is the main source of anthranilic acid in rich media (43). DHQ is a nonalkylated quinoline that is capable of being produced in both aerobic and anaerobic environments and, in a previous study, was detected in 34/80 sputum samples taken from 45 cystic fibrosis patients with histories of cultures positive for *P. aeruginosa* (31). Additionally, the well-studied quinoline, HQNO, was significantly produced in all *P. aeruginosa* strains with the exception of CDC249 (Data Set S1 in the supplemental material) and has been previously found in sputum of CF patients with
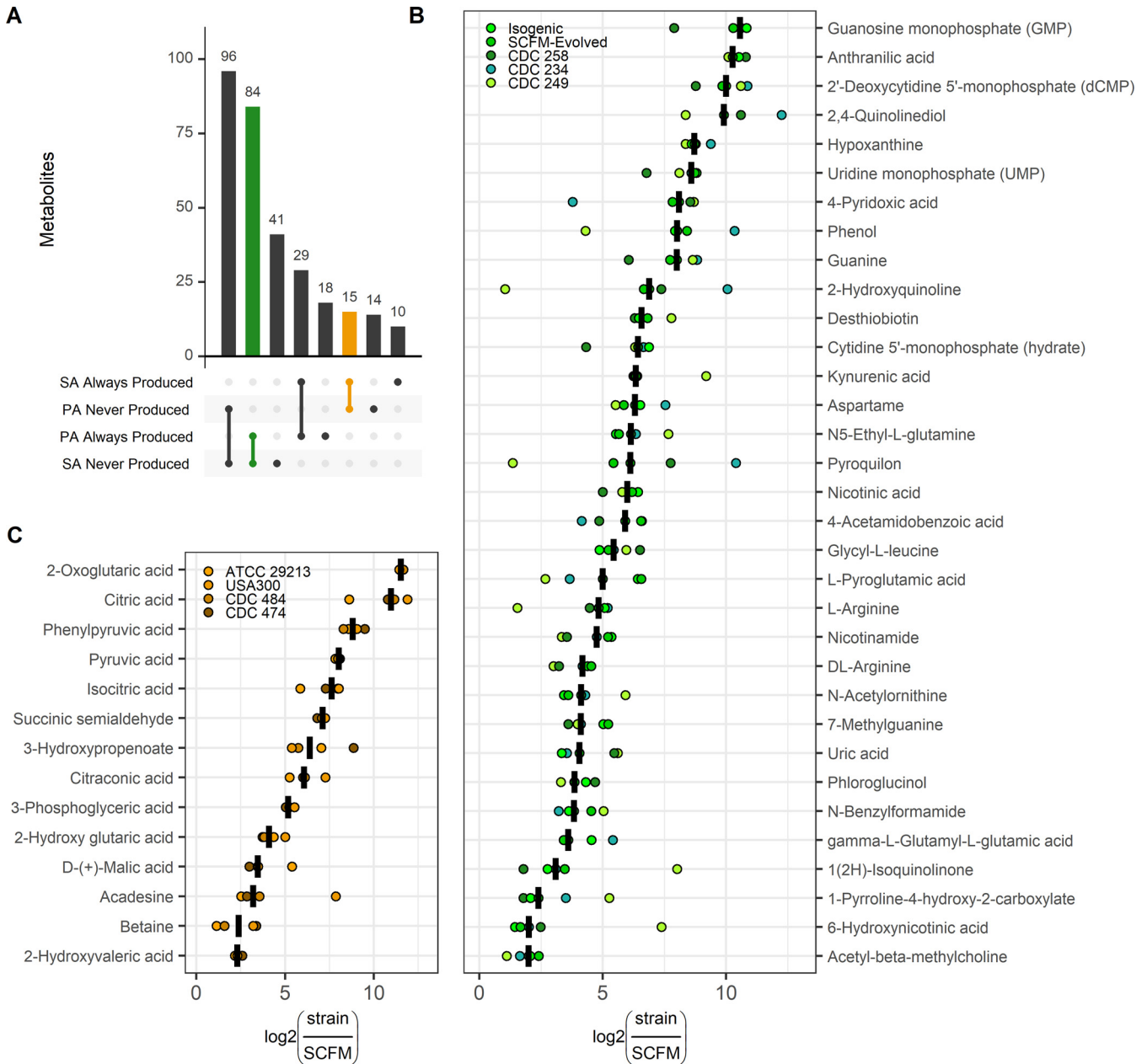
FIG 5 *P. aeruginosa* and *S. aureus* specific metabolite production in a lung-like medium. (A) Number of metabolites that were always or never significantly produced across strains of each species ($P < 0.05$, $\log_2 FC > 0$). Metabolites uniquely produced by *P. aeruginosa* strains are shown in green. Metabolites uniquely produced by *S. aureus* strains are shown in yellow. Log$_2$FCs in metabolites produced by only *P. aeruginosa* (B) or *S. aureus* (C) strains. Only metabolites with a minimum log$_2$FC of ≥1 across all strains within a species are shown. Metabolites produced by *P. aeruginosa* without an associated KEGG ID were excluded. Crossbar denotes median change of each metabolite across strains.

P. aeruginosa infections (20). Taken together, given that L-tryptophan is reliably found in CF sputum (22), PQS precursors and additional quinolines derived from L-tryptophan catabolism have the potential to be robust biomarkers of *P. aeruginosa* infection in the CF lung.

Although we identified species-specific metabolites that were produced across multiple strains and that were detected by others in CF sputum (20, 32), there are three limitations of our study that may impact the robustness of our proposed biomarkers of *P. aeruginosa* infection. First, the sources (e.g., lung, urine, etc.) of clinical isolates used in this study are unknown, and therefore, it is unclear how similar they are to isolates adapted to a CF lung environment. Second, it is possible that metabolite production may be sensitive to *in vivo* stressors (e.g., host-pathogen interactions) that were not

captured by our experimental design. For example, while absent from SCFM, mucins are highly abundant in the CF lung (45) and have been shown to impact the expression of genes involved in virulence factor production in *P. aeruginosa* (46). Finally, although our proposed biomarkers were produced across five diverse strains of *P. aeruginosa*, a single metabolite may not be sufficient to reliably detect *P. aeruginosa* infection. A stronger diagnostic could likely be developed with a signature of multiple metabolites identified in our study and from previous literature. Future studies should focus on measuring identified biomarkers in a large number of sputum samples from cystic fibrosis patients with and without *P. aeruginosa* lung infections to assess marker relevance.

In summary, we have found that *P. aeruginosa* and *S. aureus* produce distinct metabolomic profiles when grown in SCFM with limited strain-to-strain variability in significantly altered metabolites, indicating that while many metabolic interactions between the two organisms may be conserved, others may be strain-specific. Characterization of robust species-specific metabolism and intraspecies metabolic variability in physiologically relevant environments is important for the study of polymicrobial infections, especially in cases where organisms are challenging to grow in coculture *in vitro*. Furthermore, high-quality metabolomics data sets in well-established defined media are useful for interrogating cross-species and cross-strain questions of interest. A better understanding of polymicrobial interactions and more rapid and reliable species detection in sputum have the potential to greatly improve treatment of CF lung infections.

MATERIALS AND METHODS

Bacterial strains and media conditions. Three lab strains, one laboratory-adapted lab strain, and five clinical isolates were selected for metabolomics profiling (Table 1). *P. aeruginosa* strain UCBPP-PA14 (47), methicillin-sensitive *S. aureus* strain ATCC 29213, and methicillin-resistant *S. aureus* strain USA300 LAC were selected as representative laboratory strains. *P. aeruginosa* strain UCBPP-PA14 was additionally adapted to SCFM for 10 days as described below. Clinical isolates were provided by the CDC and FDA Antibiotic Resistance Isolate Bank (29; https://www.cdc.gov/drugresistance/resistance-bank/index.html). Specifically, three clinical isolates from the "*Pseudomonas aeruginosa*" panel (ID 234, ID 249, and ID 258) and two clinical isolates from the "*Staphylococcus* with Borderline Oxacillin Susceptibility" panel (ID 474 and ID 484) were selected due to their differing levels of antibiotic susceptibility.

For supernatant collection, cultures were revived from frozen on lysogeny broth (LB) agar plates, inoculated into LB liquid media, and washed in 1× Dulbecco's phosphate-buffered saline (DPBS) prior to inoculation into SCFM. SCFM was prepared and stored at 4°C as previously described (22). Stocks of SCFM components were remade as they were depleted or if precipitation or a change in color was observed. SCFM was selected over SCFM2 (48) to maximize the number of media components that could be detected in our metabolomics analysis as well as to avoid challenges associated with viscous samples (49).

Generation of an SCFM-evolved *P. aeruginosa* strain. *P. aeruginosa* strain UCBPP-PA14 (isogenic) was evolved to SCFM for 10 days prior to metabolomics profiling to create an SCFM-evolved *P. aeruginosa* isolate. Briefly, isogenic *P. aeruginosa* was streaked onto an LB agar plate and incubated for 24 h at 37°C. A single colony was inoculated into 5 ml of SCFM, and 200 μl of this culture was moved to a single well in a 96-well plate. Throughout the adaptive evolution experiment, the SCFM-evolved lineage was incubated at 37°C with shaking, and the optical density at 600 nm (OD_{600}) of the lineage was measured every 10 min (Tecan Infinite M200 Pro; Fig. S2A in the supplemental material). Every 24 h, 5 μl of culture was propagated into 195 μl of fresh SCFM, resulting in a 1:40 dilution. The remaining sample was frozen at a final concentration of 25% glycerol. This process was repeated for 10 days when growth rates had leveled out for 5 days (Fig. S2B) with the exception of between day 5 and day 6, where the lineage was revived from frozen to inspect and confirm homogeneity.

As a final check to ensure homogeneity, the day 10 SCFM-evolved *P. aeruginosa* was streaked onto an LB plate and incubated for 22 h at 37°C. A single colony was selected and inoculated into 5 ml of SCFM. This culture was grown for 26 h with shaking at 200 rpm and 37°C. Liquid culture from this sample was frozen at a final concentration of 25% glycerol, and this frozen stock was used as the SCFM-evolved lineage. The growth curves of the SCFM-evolved lineage and isogenic *P. aeruginosa* in SCFM were measured (Fig. S2C). Growth rates were calculated with the growthrates package in R (50).

Sequence analysis. Whole genomes or references of all isolates except for the SCFM-evolved *P. aeruginosa* strain were publicly available (Table 1). All genomic analyses were performed through the Pathosystems Resource Integration Center (PATRIC) (51). Raw reads of clinical isolates were assembled using the auto assembly strategy with default parameters. Assemblies of CDC isolates and ATCC 29213 were annotated using default settings. Reference genomes for UCBPP-PA14 and USA300_FPR3757 were identified within PATRIC. Finally, phylogenetic trees of *P. aeruginosa* and *S. aureus* strains were generated using the codon tree method. Default parameters were used with the exception of the number of

genes included in the analysis, which was increased to 1,000 to ensure resolution of closely related genomes.

Susceptibility profiles of bacterial strains. Susceptibility profiles of clinical isolates from the CDC and FDA Antibiotic Resistance Isolate Bank were reported as found on their database (https://www.cdc.gov/drugresistance/resistance-bank/index.html). Susceptibility profiling was performed on the remaining laboratory strains (isogenic *P. aeruginosa*, SCFM-evolved *P. aeruginosa*, ATCC 29213, and USA300) by the Clinical Microbiology Laboratory at the University of Virginia (UVA) Health System. The susceptibility of lab strains to all antibiotics was measured by broth microdilution with the exception of penicillin, which was measured using a Kirby-Bauer disk diffusion assay paired with a beta-lactamase test. Specifically, *S. aureus* laboratory strains were profiled with Vitek 2 Systems (bioMérieux Inc.), and *P. aeruginosa* laboratory strains were profiled with a Sensititre Aris 2× (Thermo Scientific). All susceptibility profiling at UVA was performed in accordance with the Clinical and Laboratory Standards Institute (CLSI), and breakpoints were consistent with the 29th edition of the CLSI M100 (52).

Collection of conditioned SCFM. Isolates were streaked from frozen stocks onto LB agar plates and incubated overnight at 37°C. Single colonies from each plate were inoculated into 5 ml of LB liquid media in 50-ml flasks and incubated at 37°C with shaking (200 rpm) overnight. Liquid cultures were washed twice in 1× DPBS and a third time in SCFM (6,000 rpm for 5 min). Washed cultures were inoculated into 25 ml of SCFM in 500-ml flasks at an OD_{600} of 0.01 ($\sim10^4$ to 10^7 CFU/ml) and were incubated at 37°C with shaking (200 rpm) for 24 h. As a control, a flask of SCFM with no bacteria was also incubated under the same conditions. Stationary cultures were centrifuged (3,000 rpm at 4°C for 20 min), and supernatants were collected, filter sterilized (22-μm PES membrane), and stored at 4°C. Colony counts were measured at the time of inoculation and just prior to collection of supernatant and reported as CFU per milliliter (Fig. S3A). The OD_{600} of each washed culture was also measured at the time of supernatant collection (Fig. S3B). Seven biological replicates were each collected on a different day, where each replicate started from an individual colony. Four batches of SCFM were used across the seven replicates.

Metabolite extraction and tandem mass spectrometry analysis of the metabolites. Supernatants were delivered fresh without freezing to the UVA Biomolecular Analysis Facility and stored at −80°C upon receipt until preparation. Approximately 150 μl of supernatants were mixed with 600 μl of ice-cold methanol and vortexed for 30 s. Samples were then centrifuged at maximum speed for 25 min at 4°C. For each sample, 600 μl (650 μl for a pooled sample) was dried in a SpeedVac and stored at −80°C until use. Prior to liquid chromatography-mass spectrometry (LC-MS) measurement, samples were reconstituted with 100 μl 0.1% formic acid and 5% methanol in water, centrifuged for 10 min, and transferred to LC vials (80 μl/sample).

Samples were analyzed in untargeted fashion by liquid chromatography-high resolution mass spectrometry (LC-HRMS). Samples were injected in randomized fashion via a Thermo Vanquish UHPLC, and separation of the metabolites was achieved using Thermo Accucore C_{18} column (Thermo Scientific; 2.1 by 100 mm, 1.5 μm) maintained at 50°C. The injection volume was 2 μl. For the 15-minute gradient, mobile phase consists of solvent A (0.1% formic acid in water) and solvent B (0.1% formic acid in methanol). The gradient was as follows: 0 to 8.0 min 50% solvent B, 8.0 to 13.0 min held at 98% solvent B, and 13.1 to 15.0 min revert to 0% solvent B to reequilibration for next injection. Spectra were acquired on Thermo ID-X Tribrid MS, using both positive and negative mode. Data were acquired in full MS mode (1 μscan) at a resolution of 120,000 with a scan range of 67 to 1,000 *m/z* at a normalized automatic gain control (AGC) target of 25%, and 50 ms of maximum injection time was allowed. RF lens amplitude was set at 35%. A heated electrospray ionization (HESI) source was operated at 3.5 kV and 2.5 kV for positive and negative modes, respectively. Ion source sheath gas was set at 35 and auxiliary gas at 7. Ion transfer tube temperature was maintained at 275°C, while vaporizer temperature was maintained at 320°C. Tandem MS was performed by applying quadrupole isolation with an isolation window of 1.6 *m/z*. Activation type was set at high-energy collisional dissociation (HCD), and masses were fragmented with HCD assisted collision energy (%) of 153,550. Fragment masses were detected by Orbitrap at a resolution of 30,000.

Raw spectra were analyzed in Compound Discoverer 3.1 with standard settings. For precursor selection, MS(n-1) precursors were selected, and signal-to-noise (S/N) threshold was set at 1.5. Retention time alignment was performed using the adaptive curve algorithm with maximum shift allowed for 2 min at a mass tolerance of 5 ppm. Compounds were detected at a mass tolerance of 5 ppm, and minimum peak intensity threshold was set at 500,000. Preferred ions were set at either [M+H] or [M−H], respectively, for positive or negative mode. Compounds were grouped at a mass tolerance of 5 ppm, and RT tolerance of 0.2 min was allowed. A quality control (QC)-based area correction was applied using a linear regression model with minimum allowable QC coverage of 50%, and maximum QC area relative standard deviation (RSD) allowed was 30%. Peak areas were normalized using constant median. Blank samples were used for detection and identification of background peaks. Compound annotations were performed by searching the ddMS² masses in mzCloud. A second search with either formula or exact mass was performed in ChemSpider, KEGG database, and an in-house database of IROA Mass Spectrometry Metabolite Library of Standards (MSMLS) (https://iroatech.com/). The in-house database contained approximate standards for 550 compounds detected in both positive and negative modes detected on the same Orbitrap mass spectrometer, using similar chromatographic separation. Metabolites were retained and considered sufficiently annotated if they met the following two conditions. First, metabolites were required to have an mzCloud or mzVault score of ≥60. Second, metabolites were required to have been verified during the second search. If a metabolite was detected in both positive and negative modes, the positive mode was kept, and the negative mode was discarded.

Quantification of glucose consumption. Glucose levels were determined using the MyQubit Amplex Red glucose assay as directed by the manufacturer (Thermo Fisher Scientific; catalog nos. A22189 and A33855; Fig. S4). Glucose measurements below the limit of detection were omitted. Glucose levels of each conditioned media sample were reported relative to unconditioned SCFM.

Metabolomics data normalization and statistical analyses. Raw peak areas for all samples and replicates were log_2 transformed and mean-centered for each high-quality metabolite. Metabolites significantly altered in conditioned SCFM relative to unconditioned SCFM were identified by performing Wilcoxon rank-sum tests on log_2-transformed, mean-centered data. The Benjamini-Hochberg method was used to correct for multiple hypothesis testing (53). Corrected P values of <0.05 were considered significant.

Log_2FCs between conditioned media and unconditioned SCFM were calculated to visualize the direction of change of significantly altered metabolites (Fig. 2A; Fig. 4B and C; Fig. 5B and C). The log_2FC was calculated as

$$\log_2 \left[\frac{\text{median}(\text{RPA}_{\text{strain}})}{\text{median}(\text{RPA}_{\text{SCFM}})} \right]$$

for each metabolite, where RPA is the raw peak area, and the medians were taken across biological replicates for each condition. Log_2FCs were used to define consumption (log_2FC < 0) and production (log_2FC > 0) of significantly altered metabolites.

Multivariate analysis, clustering, and cross-group comparisons of metabolomics data. Metabolite log_2FCs were clustered hierarchically by Euclidean distance with complete linkage (Fig. 2A). PCoA was performed on Bray-Curtis distances between raw metabolomics profiles of all samples with the ape package in R (54). The percent variance captured by each coordinate was calculated by dividing each eigenvalue by the sum of the absolute value of all eigenvalues. Cross-species and cross-strain comparisons of metabolite production and consumption were made with the UpSetR package in R (55).

Data availability. Raw metabolomics files are publicly available on the MetaboLights database (study MTBLS2105; http://www.ebi.ac.uk/metabolights/MTBLS2105) (56). All processed metabolomics data, calculated fold changes, and raw and adjusted P values are available in the supplemental material (Data Sets S1 and S2). Data and code can additionally be found at https://github.com/lauradunphy/metabolomicsSCFM.

SUPPLEMENTAL MATERIAL

Supplemental material is available online only.

DATA SET S1, CSV file, 0.3 MB.
DATA SET S2, CSV file, 3 MB.
FIG S1, JPG file, 0.2 MB.
FIG S2, JPG file, 0.3 MB.
FIG S3, JPG file, 0.4 MB.
FIG S4, JPG file, 0.1 MB.

ACKNOWLEDGMENTS

REFERENCES

1. Cystic Fibrosis Foundation. 2018. 2018 Patient Registry Annual Data Report. Cystic Fibrosis Foundation, Bethesda, Maryland.
2. Limoli DH, Hoffman LR. 2019. Help, hinder, hide and harm: what can we learn from the interactions between Pseudomonas aeruginosa and Staphylococcus aureus during respiratory infections? Thorax 74:684–692. https://doi.org/10.1136/thoraxjnl-2018-212616.
3. Hauser AR, Jain M, Bar-Meir M, McColley SA. 2011. Clinical significance of microbial infection and adaptation in cystic fibrosis. Clin Microbiol Rev 24:29–70. https://doi.org/10.1128/CMR.00036-10.
4. Maliniak ML, Stecenko AA, McCarty NA. 2016. A longitudinal analysis of chronic MRSA and Pseudomonas aeruginosa co-infection in cystic

fibrosis: a single-center study. J Cyst Fibros 15:350–356. https://doi.org/10.1016/j.jcf.2015.10.014.
5. Limoli DH, Yang J, Khansaheb MK, Helfman B, Peng L, Stecenko AA, Goldberg JB. 2016. Staphylococcus aureus and Pseudomonas aeruginosa co-infection is associated with cystic fibrosis-related diabetes and poor clinical outcomes. 6. Eur J Clin Microbiol Infect Dis 35:947–953. https://doi.org/10.1007/s10096-016-2621-0.
6. Nguyen AT, Oglesby-Sherrouse AG. 2016. Interactions between Pseudomonas aeruginosa and Staphylococcus aureus during co-cultivations and polymicrobial infections. 14. Appl Microbiol Biotechnol 100:6141–6148. https://doi.org/10.1007/s00253-016-7596-3.

7. Machan ZA, Taylor GW, Pitt TL, Cole PJ, Wilson R. 1992. 2-Heptyl-4-hydrox-yquinoline N-oxide, an antistaphylococcal agent produced by Pseudomonas aeruginosa. J Antimicrob Chemother 30:615–623. https://doi.org/10.1093/jac/30.5.615.

8. Filkins LM, Graber JA, Olson DG, Dolben EL, Lynd LR, Bhuju S, O'Toole GA. 2015. Coculture of Staphylococcus aureus with Pseudomonas aeruginosa drives S. aureus towards fermentative metabolism and reduced viability in a cystic fibrosis model. J Bacteriol 197:2252–2264. https://doi.org/10.1128/JB.00059-15.

9. Orazi G, O'Toole GA. 2017. Pseudomonas aeruginosa alters Staphylococcus aureus sensitivity to vancomycin in a biofilm model of cystic fibrosis infection. mBio 8:e00873-17. https://doi.org/10.1128/mBio.00873-17.

10. Hoffman LR, Déziel E, D'Argenio DA, Lépine F, Emerson J, McNamara S, Gibson RL, Ramsey BW, Miller SI. 2006. Selection for Staphylococcus aureus small-colony variants due to growth in the presence of Pseudomonas aeruginosa. Proc Natl Acad Sci U S A 103:19890–19895. https://doi.org/10.1073/pnas.0606756104.

11. Nixon GM, Armstrong DS, Carzino R, Carlin JB, Olinsky A, Robertson CF, Grimwood K. 2001. Clinical outcome after early Pseudomonas aeruginosa infection in cystic fibrosis. J Pediatr 138:699–704. https://doi.org/10.1067/mpd.2001.112897.

12. Medlock GL, Carey MA, McDuffie DG, Mundy MB, Giallourou N, Swann JR, Kolling GL, Papin JA. 2018. Inferring metabolic mechanisms of interaction within a defined gut microbiota. Cell Syst 7:245–257.e7. https://doi.org/10.1016/j.cels.2018.08.003.

13. Biggs MB, Medlock GL, Moutinho TJ, Lees HJ, Swann JR, Kolling GL, Papin JA. 2017. Systems-level metabolism of the altered Schaedler flora, a complete gut microbiota. ISME J 11:426–438. https://doi.org/10.1038/ismej.2016.130.

14. Jenior ML, Leslie JL, Young VB, Schloss PD. 2018. Clostridium difficile alters the structure and metabolism of distinct cecal microbiomes during initial infection to promote sustained colonization. mSphere 3:e00261-18. https://doi.org/10.1128/mSphere.00261-18.

15. Frydenlund Michelsen C, Hossein Khademi SM, Krogh Johansen H, Ingmer H, Dorrestein PC, Jelsbak L. 2016. Evolution of metabolic divergence in Pseudomonas aeruginosa during long-term infection facilitates a proto-cooperative interspecies interaction. ISME J 10:1323–1336. https://doi.org/10.1038/ismej.2015.220.

16. Voge NV, Perera R, Mahapatra S, Gresh L, Balmaseda A, Loroño-Pino MA, Hopf-Jannasch AS, Belisle JT, Harris E, Blair CD, Beaty BJ. 2016. Metabolomics-based discovery of small molecule biomarkers in serum associated with dengue virus infections and disease outcomes. PLoS Negl Trop Dis 10:e0004449. https://doi.org/10.1371/journal.pntd.0004449.

17. Godoy-Vitorino F, Ortiz-Morales G, Romaguera J, Sanchez MM, Martinez-Ferrer M, Chorna N. 2018. Discriminating high-risk cervical human papilloma virus infections with urinary biomarkers via non-targeted GC-MS-based metabolomics. PLoS One 13:e0209936. https://doi.org/10.1371/journal.pone.0209936.

18. Abdelrazig S, Ortori CA, Davey G, Deressa W, Mulleta D, Barrett DA, Amberbir A, Fogarty AW. 2017. A metabolomic analytical approach permits identification of urinary biomarkers for Plasmodium falciparum infection: a case–control study. Malar J 16:229. https://doi.org/10.1186/s12936-017-1875-z.

19. Weiner J, Maertzdorf J, Sutherland JS, Duffy FJ, Thompson E, Suliman S, McEwen G, Thiel B, Parida SK, Zyla J, Hanekom WA, Mohney RP, Boom WH, Mayanja-Kizza H, Howe R, Dockrell HM, Ottenhoff THM, Scriba TJ, Zak DE, Walzl G, Kaufmann SHE, The GC6-74 Consortium. 2018. Metabolite changes in blood predict the onset of tuberculosis. Nat Commun 9:5208. https://doi.org/10.1038/s41467-018-07635-7.

20. Quinn RA, Phelan VV, Whiteson KL, Garg N, Bailey BA, Lim YW, Conrad DJ, Dorrestein PC, Rohwer FL. 2016. Microbial, host and xenobiotic diversity in the cystic fibrosis sputum metabolome. ISME J 10:1483–1498. https://doi.org/10.1038/ismej.2015.207.

21. Raghuvanshi R, Vasco K, Vázquez-Baeza Y, Jiang L, Morton JT, Li D, Gonzalez A, Goldasich LD, Humphrey G, Ackermann G, Swafford AD, Conrad D, Knight R, Dorrestein PC, Quinn RA. 2020. High-resolution longitudinal dynamics of the cystic fibrosis sputum microbiome and metabolome through antibiotic therapy. mSystems 5:e00292-20. https://doi.org/10.1128/mSystems.00292-20.

22. Palmer KL, Aye LM, Whiteley M. 2007. Nutritional cues control Pseudomonas aeruginosa multicellular behavior in cystic fibrosis sputum. J Bacteriol 189:8079–8087. https://doi.org/10.1128/JB.01138-07.

23. Behrends V, Geier B, Williams HD, Bundy JG. 2013. Direct assessment of metabolite utilization by Pseudomonas aeruginosa during growth on artificial sputum medium. Appl Environ Microbiol 79:2467–2470. https://doi.org/10.1128/AEM.03609-12.

24. Frimmersdorf E, Horatzek S, Pelnikevich A, Wiehlmann L, Schomburg D. 2010. How Pseudomonas aeruginosa adapts to various environments: a metabolomic approach. Environ Microbiol 12:1734–1747. https://doi.org/10.1111/j.1462-2920.2010.02253.x.

25. Mielko KA, Jabłoński SJ, Milczewska J, Sands D, Łukaszewicz M, Młynarz P. 2019. Metabolomic studies of Pseudomonas aeruginosa. World J Microbiol Biotechnol 35:178. https://doi.org/10.1007/s11274-019-2739-1.

26. Moyne O, Castelli F, Bicout DJ, Boccard J, Camara B, Cournoyer B, Faudry E, Terrier S, Hannani D, Huot-Marchand S, Léger C, Maurin M, Ngo T-D, Plazy C, Quinn RA, Attree I, Fenaille F, Toussaint B, Le Gouëllec A. 2021. Metabotypes of Pseudomonas aeruginosa correlate with antibiotic resistance, virulence and clinical outcome in cystic fibrosis chronic infections. Metabolites 11:63. https://doi.org/10.3390/metabo11020063.

27. Mielko KA, Jabłoński SJ, Wojtowicz W, Milczewska J, Sands D, Łukaszewicz M, Młynarz P. 2020. Possible metabolic switch between environmental and pathogenic Pseudomonas aeruginosa strains: 1H NMR based metabolomics study. J Pharm Biomed Anal 188:113369. https://doi.org/10.1016/j.jpba.2020.113369.

28. Briaud P, Camus L, Bastien S, Doléans-Jordheim A, Vandenesch F, Moreau K. 2019. Coexistence with Pseudomonas aeruginosa alters Staphylococcus aureus transcriptome, antibiotic resistance and internalization into epithelial cells. Sci Rep 9:16564. https://doi.org/10.1038/s41598-019-52975-z.

29. Lutgring JD, Machado M-J, Benahmed FH, Conville P, Shawar RM, Patel J, Brown AC. 2018. FDA-CDC Antimicrobial Resistance Isolate Bank: a publicly available resource to support research, development, and regulatory requirements. J Clin Microbiol 56:e01415-17. https://doi.org/10.1128/JCM.01415-17.

30. Mashburn LM, Jett AM, Akins DR, Whiteley M. 2005. Staphylococcus aureus serves as an iron source for Pseudomonas aeruginosa during in vivo coculture. J Bacteriol 187:554–566. https://doi.org/10.1128/JB.187.2.554-566.2005.

31. Gruber JD, Chen W, Parnham S, Beauchesne K, Moeller P, Flume PA, Zhang Y-M. 2016. The role of 2,4-dihydroxyquinoline (DHQ) in Pseudomonas aeruginosa pathogenicity. PeerJ 4:e1495. https://doi.org/10.7717/peerj.1495.

32. Bortolotti P, Hennart B, Thieffry C, Jausions G, Faure E, Grandjean T, Thepaut M, Dessein R, Allorge D, Guery BP, Faure K, Kipnis E, Toussaint B, Le Gouellec A. 2016. Tryptophan catabolism in Pseudomonas aeruginosa and potential for inter-kingdom relationship. BMC Microbiol 16:137. https://doi.org/10.1186/s12866-016-0756-x.

33. Gupta A, Dwivedi M, Gowda GAN, Ayyagari A, Mahdi AA, Bhandari M, Khetrapal CL. 2005. 1H NMR spectroscopy in the diagnosis of Pseudomonas aeruginosa-induced urinary tract infection. NMR Biomed 18:293–299. https://doi.org/10.1002/nbm.957.

34. Halsey CR, Lei S, Wax JK, Lehman MK, Nuxoll AS, Steinke L, Sadykov M, Powers R, Fey PD. 2017. Amino acid catabolism in Staphylococcus aureus and the function of carbon catabolite repression. mBio 8:e01434-16. https://doi.org/10.1128/mBio.01434-16.

35. Liebeke M, Dörries K, Zühlke D, Bernhardt J, Fuchs S, Pané-Farré J, Engelmann S, Völker U, Bode R, Dandekar T, Lindequist U, Hecker M, Lalk M. 2011. A metabolomics and proteomics study of the adaptation of Staphylococcus aureus to glucose starvation. Mol Biosyst 7:1241–1253. https://doi.org/10.1039/c0mb00315h.

36. Dunphy LJ, Yen P, Papin JA, 2019. Integrated experimental and computational analyses reveal differential metabolic functionality in antibiotic-resistant Pseudomonas aeruginosa. Cell Syst 8:3–14.e3. https://doi.org/10.1016/j.cels.2018.12.002.

37. Ibberson CB, Whiteley M, 2019. The Staphylococcus aureus transcriptome during cystic fibrosis lung infection. mBio 10:e02774-19. https://doi.org/10.1128/mBio.02774-19.

38. Limoli DH, Whitfield GB, Kitao T, Ivey ML, Davis MR, Grahl N, Hogan DA, Rahme LG, Howell PL, O'Toole GA, Goldberg JB. 2017. Pseudomonas aeruginosa alginate overproduction promotes coexistence with Staphylococcus aureus in a model of cystic fibrosis respiratory infection. mBio 8:e00186-17. https://doi.org/10.1128/mBio.00186-17.

39. Gao C-H, Cao H, Cai P, Sørensen SJ. 2021. The initial inoculation ratio regulates bacterial coculture interactions and metabolic capacity. ISME J 15:29–40. https://doi.org/10.1038/s41396-020-00751-7.

40. Coleman JP, Hudson LL, McKnight SL, Farrow JM, Calfee MW, Lindsey CA, Pesci EC. 2008. Pseudomonas aeruginosa PqsA Is an anthranilate-coenzyme A ligase. J Bacteriol 190:1247–1255. https://doi.org/10.1128/JB.01140-07.

41. Déziel E, Lépine F, Milot S, He J, Mindrinos MN, Tompkins RG, Rahme LG. 2004. Analysis of Pseudomonas aeruginosa 4-hydroxy-2-alkylquinolines (HAQs) reveals a role for 4-hydroxy-2-heptylquinoline in cell-to-cell communication. Proc Natl Acad Sci U S A 101:1339–1344. https://doi.org/10.1073/pnas.0307694100.

42. Zhang Y-M, Frank MW, Zhu K, Mayasundari A, Rock CO. 2008. PqsD is responsible for the synthesis of 2,4-dihydroxyquinoline, an extracellular metabolite produced by Pseudomonas aeruginosa. J Biol Chem 283:28788–28794. https://doi.org/10.1074/jbc.M804555200.

43. Farrow JM, Pesci EC. 2007. Two distinct pathways supply anthranilate as a precursor of the Pseudomonas quinolone signal. J Bacteriol 189:3425–3433. https://doi.org/10.1128/JB.00209-07.

44. Palmer KL, Mashburn LM, Singh PK, Whiteley M. 2005. Cystic fibrosis sputum supports growth and cues key aspects of Pseudomonas aeruginosa physiology. J Bacteriol 187:5267–5277. https://doi.org/10.1128/JB.187.15.5267-5277.2005.

45. Morrison CB, Markovetz MR, Ehre C. 2019. Mucus, mucins, and cystic fibrosis. Pediatr Pulmonol 54:S84–S96. https://doi.org/10.1002/ppul.24530.

46. Wheeler KM, Cárcamo-Oyarce G, Turner BS, Dellos-Nolan S, Co JY, Lehoux S, Cummings RD, Wozniak DJ, Ribbeck K. 2019. Mucin glycans attenuate the virulence of Pseudomonas aeruginosa in infection. Nat Microbiol 4:2146–2154. https://doi.org/10.1038/s41564-019-0581-8.

47. Liberati NT, Urbach JM, Miyata S, Lee DG, Drenkard E, Wu G, Villanueva J, Wei T, Ausubel FM. 2006. An ordered, nonredundant library of Pseudomonas aeruginosa strain PA14 transposon insertion mutants. Proc Natl Acad Sci U S A 103:2833–2838. https://doi.org/10.1073/pnas.0511100103.

48. Turner KH, Wessel AK, Palmer GC, Murray JL, Whiteley M. 2015. Essential genome of Pseudomonas aeruginosa in cystic fibrosis sputum. Proc Natl Acad Sci U S A 112:4110–4115. https://doi.org/10.1073/pnas.1419677112.

49. La Rosa R, Johansen HK, Molin S. 2019. Adapting to the airways: metabolic requirements of Pseudomonas aeruginosa during the infection of cystic fibrosis patients. Metabolites 9:234. https://doi.org/10.3390/metabo9100234.

50. Petzoldt T. 2019. growthrates: estimate growth rates from experimental data. https://cran.r-project.org/web/packages/growthrates/index.html.

51. Wattam AR, Davis JJ, Assaf R, Boisvert S, Brettin T, Bun C, Conrad N, Dietrich EM, Disz T, Gabbard JL, Gerdes S, Henry CS, Kenyon RW, Machi D, Mao C, Nordberg EK, Olsen GJ, Murphy-Olson DE, Olson R, Overbeek R, Parrello B, Pusch GD, Shukla M, Vonstein V, Warren A, Xia F, Yoo H, Stevens RL. 2017. Improvements to PATRIC, the all-bacterial Bioinformatics Database and Analysis Resource Center. Nucleic Acids Res 45:D535–D542. https://doi.org/10.1093/nar/gkw1017.

52. Clinical and Laboratory Standards Institute. 2019. performance standards for antimicrobial susceptibility testing, 29th ed. CLSI supplement M100. Clinical and Laboratory Standards Institute, Wayne, PA.

53. Benjamini Y, Hochberg Y. 1995. Controlling the false discovery rate: a practical and powerful approach to multiple testing. J R Stat Soc Ser B Methodol 57:289–300. https://doi.org/10.1111/j.2517-6161.1995.tb02031.x.

54. Paradis E, Schliep K. 2019. ape 5.0: an environment for modern phylogenetics and evolutionary analyses in R. Bioinformatics 35:526–528. https://doi.org/10.1093/bioinformatics/bty633.

55. Conway JR, Lex A, Gehlenborg N. 2017. UpSetR: an R package for the visualization of intersecting sets and their properties. Bioinforma Oxf Engl 33:2938–2940. https://doi.org/10.1093/bioinformatics/btx364.

56. Haug K, Cochrane K, Nainala VC, Williams M, Chang J, Jayaseelan KV, O'Donovan C. 2020. MetaboLights: a resource evolving in response to the needs of its scientific community. Nucleic Acids Res 48:D440–D444. https://doi.org/10.1093/nar/gkz1019.

57. Lee DG, Urbach JM, Wu G, Liberati NT, Feinbaum RL, Miyata S, Diggins LT, He J, Saucier M, Déziel E, Friedman L, Li L, Grills G, Montgomery K, Kucherlapati R, Rahme LG, Ausubel FM. 2006. Genomic analysis reveals that Pseudomonas aeruginosa virulence is combinatorial. Genome Biol 7:R90. https://doi.org/10.1186/gb-2006-7-10-r90.

58. Liu A, Archer AM, Biggs MB, Papin JA. 2017. Growth-altering microbial interactions are responsive to chemical context. PLoS One 12:e0164919. https://doi.org/10.1371/journal.pone.0164919.

59. Soni I, Chakrapani H, Chopra S. 2015. Draft genome sequence of methicillin-sensitive Staphylococcus aureus ATCC 29213. Genome Announc 3:e01095-15. https://doi.org/10.1128/genomeA.01095-15.

60. Diep BA, Gill SR, Chang RF, Phan TH, Chen JH, Davidson MG, Lin F, Lin J, Carleton HA, Mongodin EF, Sensabaugh GF, Perdreau-Remington F. 2006. Complete genome sequence of USA300, an epidemic clone of community-acquired meticillin-resistant Staphylococcus aureus. Lancet Lond Engl 367:731–739. https://doi.org/10.1016/S0140-6736(06)68231-7.